An Electron Spin-Echo Envelope Modulation Study of Cu(II)-Doped Single Crystals of L-Histidine Hydrochloride Monohydrate

Michael J. Colaneri* and Jack Peisach

Contribution from the Department of Molecular Pharmacology, Albert Einstein College of Medicine of Yeshiva University, Bronx, New York 10461. *Received December 4, 1991*

Abstract: Single-crystal electron spin-echo envelope modulation (ESEEM) spectroscopy was utilized to accurately measure the ^{14}N hyperfine and quadrupole coupling tensors for the remote or noncoordinating nitrogen of histidine imidazole ligated to copper in doped L-histidine $HCl\cdot H_2O$. The anisotropic part of the ^{14}N hyperfine tensor is of the form $(A, 0, -A)$. Nevertheless, the hyperfine tensor could be simply modeled by a multipoint representation of delocalized spin density both in the postulated copper unpaired orbital and on the imidazole moiety itself. Hence, the anisotropic part of the remote nitrogen hyperfine tensor may be a better probe of the ligand geometry and copper unpaired orbital than the isotropic hyperfine component. An analysis invoking the Townes-Dailey approximation was applied to the derived quadrupole tensor of the remote nitrogen of imidazole in Cu(II)-doped L-histidine $HCl\cdot H_2O$. This analysis was extended to include known quadrupole coupling parameters of the amino nitrogen in imidazole compounds that have also been the subject of neutron diffraction studies. A linear relationship was found between the ^{14}N valence occupancy in the N-H fragment and the inverse cube of the corresponding N-H bond lengths. Such an empirical relationship has the potential for accurately predicting N-H bond lengths in imidazole compounds from a simple analysis of the quadrupole tensor parameters.

Introduction

Of recent interest in this laboratory is the analysis of the imidazole amino ^{14}N nuclear quadrupole interaction which has been postulated as being significantly affected by hydrogen-bonding interactions.[1-9] The nuclear electric-quadrupole coupling interaction provides information on the electrostatic field gradient at the nuclear position, from which important bonding characteristics can be deduced.[10] As has been suggested by electron spin-echo envelope modulation (ESEEM) frozen solution studies, the quadrupole coupling parameters of the remote or noncoordinating nitrogen in a series of imidazole model compounds ligated to copper appear to be correlated, in part, with hydrogen bonding.[9] The extension of this hypothesis to ESEEM results obtained from protein frozen solution samples, which show a variation in the quadrupole parameters of the remote nitrogen of histidyl imidazole, gave predictions concerning the relative hydrophobic environment of the imidazole moiety in copper binding sites.[9] In contrast, of all the copper bound histidine model systems studied by ESEEM to date,[9,11] none have shown a large deviation of the remote nitrogen quadrupole coupling parameters from those found by nuclear quadrupole resonances (NQR) for solid imidazole.[2,5,12,13] Hence, the present work was undertaken in an attempt to clearly demonstrate the existence of this parametric variation in a more biologically relevant ligand model system, namely copper doped into L-histidine hydrochloride monohydrate. As has been shown by ESEEM studies on Cu(II)-doped zinc(II) bis(1,2-dimethylimidazole) dichloride, the greater precision in measuring the coupling tensors afforded by single crystal studies results in an unambiguous assignment of the remote nitrogen quadrupole tensor principal directions.[14] This assignment is essential in order to correctly assess the nitrogen valence orbital occupancies.

A previous electron paramagnetic resonance (EPR) and polarized optical absorption spectral study of Cu(II)-doped L-histidine $HCl\cdot H_2O$ suggested that the copper unpaired wave function has predominantly a dz^2 angular function.[15] The copper site has been postulated as being interstitial between two chloride anions, oxygens from water and carboxyl groups, and nitrogens from two histidines, one each from the imidazole moiety (N3) and the amino group (N1). The z axes was tentatively defined as roughly along the crystallographic b axis, although not completely along the N1···N3 direction in the crystal structure. A later study on this system in which the g tensor and copper hyperfine were reanalyzed and the ligand hyperfine and quadrupole coupling tensors were determined by electron-nuclear double resonance (ENDOR) measurements only slightly modified the dope site.[16]

The EPR parameters for Cu(II)-doped L-histidine $HCl\cdot H_2O$ ($g_x = 2.256$, $g_y = 2.167$, $g_z = 2.007$ and $A_x = 178.5$ MHz, $A_y = 41.7$ MHz, $A_z = 405.7$ MHz)[16] are similar to those found in frozen solution studies of the Cu_B site in cytochrome c oxidase[17] and of the partially reduced type 3 copper center of tree laccase ($g_1 = 2.277$, $g_2 = 2.15$, $g_3 = 2.03$ and $A_1 = 396$ MHz, $A_2 = 0$ MHz, $A_3 = 218$ MHz[17c]).[17] However, unlike Cu(II)-doped zinc(II) bis(1,2-dimethylimidazole) dichloride, which has been shown to be a good model for type 1[18] copper sites by a combination of crystallographic results, single-crystal EPR, optical analysis, and theoretical calculations in comparison with the blue copper protein, plastocyanin,[19] it is unclear whether the postulated

(1) Hunt M. J.; Mackay, A. L. *J. Magn. Reson.* **1974**, *15*, 402.
(2) (a) Ashby, C. I. H.; Cheng, C. P.; Brown, T. L. *J. Am. Chem. Soc.* **1978**, *100*, 6057. (b) Ashby, C. I. H.; Paton, W. F.; Brown, T. L. *J. Am. Chem. Soc.* **1980**, *102*, 2990.
(3) Christen, D.; Griffiths, J. H.; Sheridan, J. *Z. Naturforsch.* **1982**, *37a*, 1378.
(4) Palmer, M. H.; Scott, F. E.; Smith, J. A. S. *Chem. Phys.* **1983**, *74*, 9.
(5) Garcia, M. L. S.; Smith, J. A. S.; Bavin, P. M. G.; Ganellin, C. R. *J. Chem. Soc., Perkin Trans. 2* **1983**, 1391.
(6) Hiyama, Y.; Keiter, E. A.; Brown, T. L. *J. Magn. Reson.* **1986**, *67*, 202.
(7) McDowell, C. A.; Naito, A.; Sastry, D. L.; Takegoshi, K. *J. Magn. Reson.* **1986**, *69*, 283.
(8) Palmer, M. H. *Chem. Phys.* **1987**, 1150, 207.
(9) Jiang, F.; McCracken, J.; Peisach, J. *J. Am. Chem. Soc.* **1990**, *112*, 9035.
(10) Lucken, E. A. C. *Nuclear Quadrupole Coupling Constants*; Academic Press: New York, 1969.
(11) Goldfarb, D.; Fauth, J.-M.; Tor, Y.; Shanzer, A. *J. Am. Chem. Soc.* **1991**, *113*, 1941.
(12) (a) Koo, J.; Hsieh, Y.-N. *Chem. Phys. Lett.* **1971**, *9*, 238. (b) Edmonds, D. T.; Speight, P. A. *J. Magn. Reson.* **1972**, *6*, 265.
(13) Hunt, M. J.; Mackay, A. L.; Edmonds, D. T. *Chem. Phys. Lett.* **1975**, *34*, 473.
(14) Colaneri, M. J.; Potenza, J. A.; Schugar, H. J.; Peisach, J. *J. Am. Chem. Soc.* **1990**, *112*, 9451.
(15) Hirasawa, R.; Kon, H. *J. Chem. Phys.* **1972**, *56*, 4467.
(16) McDowell, C. A.; Naito, A.; Sastry, D. L.; Cui, Y. U.; Sha, K.; Yu, S. X. *J. Mol. Struct.* **1989**, *185*, 361.
(17) (a) Reinhammar, B.; Malkin, R.; Jensen, P.; Karlsson, B.; Andreasson, L.-E.; Aasa, R.; Vanngard, T.; Malmstrom, B. G. *J. Biol. Chem.* **1980**, *11*, 5000. (b) Reinhammar, B. J. *Inorg. Biochem.* **1983**, *18*, 113. (c) Cline, J.; Reinhammar, B.; Jensen, P.; Venters, R.; Hoffman, B. M. *J. Biol. Chem.* **1983**, *258*, 5124.
(18) Malkin, R.; Malmström, B. G. *Adv. Enzymol.* **1970**, *33*, 177.
(19) Gewirth, A. A.; Cohen, S. L.; Schugar, H. J.; Solomon, E. I. *Inorg. Chem.* **1987**, *26*, 1133.

0002-7863/92/1514-5335$03.00/0

unpaired metal orbital in the Cu(II)-doped L-histidine $HCl \cdot H_2O$ system is similar to that in any known protein copper site. On the other hand, the present complex more closely resembles the situation found in proteins where L-histidine is found to routinely ligate to copper.[20-23] In addition, copper is postulated to coordinate to the ϵ nitrogen of imidazole (i.e., the imidazole nitrogen furthest from the histidine C_β, see I) which is similar to the

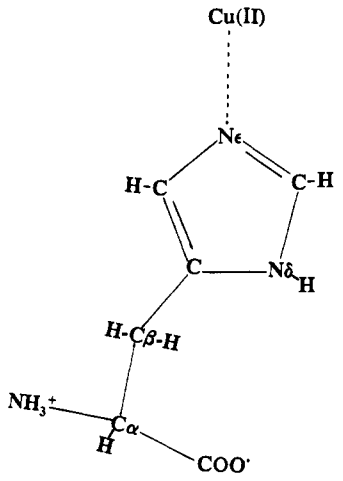

I

arrangement found in the type 2[18] sites of ascorbate oxidase[20] and galactose oxidase.[21] This ligation arrangement is to be compared with that found in the type 1 sites of blue copper proteins[22] and of a multicopper oxidase[20] where the δ histidine nitrogen rather than the ϵ histidine nitrogen binds to the copper. The ESEEM spectroscopic parameters for the noncoordinating nitrogen (N_δ) of imidazole in histidine are of interest in view of the above mentioned remote ^{14}N quadrupole coupling variations observed in protein frozen samples which have been previously reported as appearing to depend on the type of copper site.[23f] The determination of the remote ^{14}N hyperfine interaction when the imidazole group binds near or along the copper spin occupied dz^2 orbital direction is also of general interest in terms of the spectral parametric dependencies on coordination geometry.

Experimental Section

Single crystals of Cu(II)-doped L-histidine hydrochloride monohydrate were grown by slow evaporation of a saturated aqueous solution of L-histidine hydrochloride monohydrate (Aldrich) containing 1 molar percent of cupric chloride (Aldrich). The rhombic EPR spectra of crushed crystals was consistent with that of the previously characterized copper species.[15]

L-Histidine $HCl \cdot H_2O$ crystallizes in space group $P2_12_12_1$ with four molecules in the unit cell.[24,25] The crystalline axes were clearly distinguishable given the previous morphological and EPR descriptions,[15] and these axes were subsequently used as a reference for the data collection. Crystals were affixed with vacuum grease (Dow Corning) to the wall of an X-band TE_{110} rectangular reflection cavity described by Mims.[26] Crystals were in turn mounted with their crystallographic *a*, *b*, and *c* axes parallel to the magnetic field rotation axis. Crystal mounting uncertainties were $<\pm 3°$ as estimated from repetitive measurements. Echo envelope decay curves were typically acquired at 5° intervals of the magnetic field orientation.

An electron spin–echo spectrometer operating at X-band and described previously was utilized for the generation of electron spin–echoes and detection of the stimulated (3-pulse) echo envelope decay.[27] The echo envelope decay patterns were measured, fourier transformed, and plotted as described previously.[14] The ^{14}N modulation frequencies thus obtained were followed as a function of magnetic field orientation in the three orthogonal planes. These data were used to least-squares fit ^{14}N coupling parameters to a spin hamiltonian

$$\mathcal{H} = \beta \mathbf{S}\cdot\mathbf{g}\cdot\mathbf{H} + \mathbf{I}^{Cu}\cdot\mathbf{A}^{Cu}\cdot\mathbf{S} - g_n^{Cu}\beta_n\mathbf{H}\cdot\mathbf{I}^{Cu} + \mathbf{I}^{N}\cdot\mathbf{A}^{N}\cdot\mathbf{S} - g_n^{N}\beta_n\mathbf{H}\cdot\mathbf{I}^{N} + \mathbf{I}^{N}\cdot\mathbf{Q}^{N}\cdot\mathbf{I}^{N}$$

by methods described earlier.[14,28] Adjustable parameters included the six nitrogen hyperfine ($\mathbf{A}^N$) components and five independent elements of the traceless quadrupole tensor ($\mathbf{Q}^N$). Other terms in the above equation have been explained elsewhere.[29] The **g** tensor and copper hyperfine tensor ($\mathbf{A}^{Cu}$) utilized in eq 1 were obtained from McDowell et al.[16] Confirming earlier approximate analyses, the inclusion of the copper hyperfine parameters in the least-squares refinement only slightly affects the nitrogen coupling parameters.[14]

Fourier transform ESEEM simulations at discrete magnetic field orientations were accomplished by methods described previously.[14]

Table I. The Remote ^{14}N Hyperfine and Quadrupole Coupling Tensors in Imidazole Obtained from Cu(II)-Doped L-Histidine $HCl \cdot H_2O$[a]

	principal values (MHz)	a_{iso}	direction cosines		
			a	*b*	*c*
		Hyperfine Tensor			
N2	1.72		−0.3421	0.8678	0.3604
	1.26	1.35	0.3150	−0.2554	0.9141
	1.07		0.8853	0.4263	−0.1859
		Quadrupole Tensor			
N2	0.70		−0.4049	0.6625	−0.6302
	−0.12		−0.1741	0.6208	0.7644
	−0.58		0.8976	0.4192	−0.1360

[a] a_{iso} is the isotropic component of the hyperfine tensor. Estimated uncertainties in the tensor parameters are ≤ 0.0037 MHz for the principal values and $\leq 2°$ for the principal directions. The tensors were assigned to the histidine imidazole N2 as discussed in the text.

Results

The Determination of the ^{14}N Coupling Tensors. Fourier cosine transforms of the electron spin–echo envelope decays (FT-ESEEM) obtained when the applied magnetic field (**H**) was aligned along the crystallographic *a*, *b*, and *c* axis directions are depicted in Figure 1. Low-intensity lines in these spectra were attributed to minor species in the copper-doped crystal and were subsequently ignored (compare experimental and simulated spectra in Figure 1). The orientational dependencies of the ^{14}N modulation

(20) Messerschmidt, A.; Rossi, A.; Ladenstein, R.; Huber, R.; Bolognesi, M.; Gatti, G.; Marchesini, A.; Petruzzelli, R.; Finazzi-Agro, A. *J. Mol. Biol.* **1989**, *206*, 513.
(21) Ito, N.; Phillips, S. E. V.; Stevens, C.; Ogel, Z. B.; McPherson, M. J.; Keen, J. N.; Yadav, K. D. S.; Knowles, P. F. *Nature* **1991**, *350*, 87.
(22) (a) Petratos, K.; Dauter, Z.; Wilson, K. S. *Acta Crystallogr.* **1988**, *B44*, 628. (b) Adman, E. T.; Turley, S.; Bramson, R.; Petratos, K.; Banner, D.; Tsernoglou, D.; Beppu, T.; Watanabe, H. *J. Biol. Chem.* **1989**, *264*, 87. (c) Guss, J. M.; Merritt, E. A.; Phizackerley, R. P.; Hedman, B.; Murata, M.; Hodgson, K. O.; Freeman, H. C. *Science* **1988**, *241*, 806. (d) Korszun, Z. R. *J. Mol. Biol.* **1987**, *196*, 413. (e) Adman, E. T.; Stenkamp, R. E.; Sieker, L. C.; Jensen, L. H. *J. Mol. Biol.* **1978**, *123*, 35. (f) Adman, E. T.; Jensen, L. H. *Isr. J. Chem.* **1981**, *21*, 8. (g) Colman, P. M.; Freeman, H. C.; Guss, J. M.; Murata, M.; Norris, V. A.; Ramshaw, J. A. M.; Venkatappa, M. P. *Nature* **1978**, *272*, 319. (h) Guss, J. M.; Freeman, H. C. *J. Mol. Biol.* **1983**, *169*, 521. (i) Church, W. B.; Guss, J. M.; Potter, J. J.; Freeman, H. C. *J. Biol. Chem.* **1986**, *261*, 234. (j) Norris, G. E.; Anderson, B. F.; Baker, E. N.; Rumball, S. V. *J. Mol. Biol.* **1979**, *135*, 309. (k) Norris, G. E.; Anderson, B. F.; Baker, E. N. *J. Mol. Biol.* **1983**, *165*, 501. (l) Norris, G. E.; Anderson, B. F.; Baker, E. N. *J. Am. Chem. Soc.* **1986**, *108*, 2784. (m) Baker, E. N. *J. Mol. Biol.* **1988**, *203*, 1071.
(23) (a) Mims, W. B.; Peisach, J. *Biochemistry* **1976**, *15*, 3863. (b) Mondovi, B.; Graziani, M. T.; Mims, W. B.; Oltzik, R.; Peisach, J. *Biochemistry* **1977**, *16*, 4198. (c) Mims, W. B.; Peisach, J. *J. Biol. Chem.* **1979**, *254*, 4321. (d) Kosman, D. J.; Peisach, J.; Mims, W. B. *Biochemistry* **1980**, *19*, 1304. (e) Fee, J. A.; Peisach, J.; Mims, W. B. *J. Biol. Chem.* **1981**, *256*, 1910. (f) Avigliano, L.; Davis, J. L.; Graziani, M. T.; Marchesini, A.; Mims, W. B.; Mondovi, B.; Peisach, J. *FEBS Lett.* **1981**, *136*, 80. (g) Zweier, J. L.; Peisach, J.; Mims, W. B. *J. Biol. Chem.* **1982**, *257*, 10314. (h) McCracken, J.; Desai, P. R.; Papadopoulos, N. J.; Villafranca, J. J.; Peisach, J. *Biochemistry* **1988**, *27*, 4133. (i) McCracken, J.; Pember, S.; Benkovic, S. J.; Villafranca, J. J.; Miller, R. J.; Peisach, J. *J. Am. Chem. Soc.* **1988**, *110*, 1069.
(24) (a) Donohue, J.; Caron, A. *Acta Crystallogr.* **1964**, *17*, 1178. (b) Donohue, J.; Lavine, L. R.; Rollett, J. S. *Acta Crystallogr.* **1956**, *9*, 655. (c) Oda, K.; Koyama, H. *Acta Crystallogr.* **1972**, *B28*, 639.
(25) Fuess, H.; Hohlwein, D.; Mason, S. A. *Acta Crystallogr.* **1977**, *B33*, 654.
(26) Mims, W. B. *Phys. Rev.* **1964**, *133*, A835.
(27) McCracken, J.; Peisach, J.; Dooley, D. M. *J. Am. Chem. Soc.* **1987**, *109*, 4064.
(28) Colaneri, M. J.; Box, H. C. *J. Chem. Phys.* **1986**, *84*, 1926.
(29) Wertz, J. E.; Bolton, J. R. In *Electron Spin Resonance: Elementary Theory and Practical Applications*; McGraw-Hill, Inc., New York, 1972.

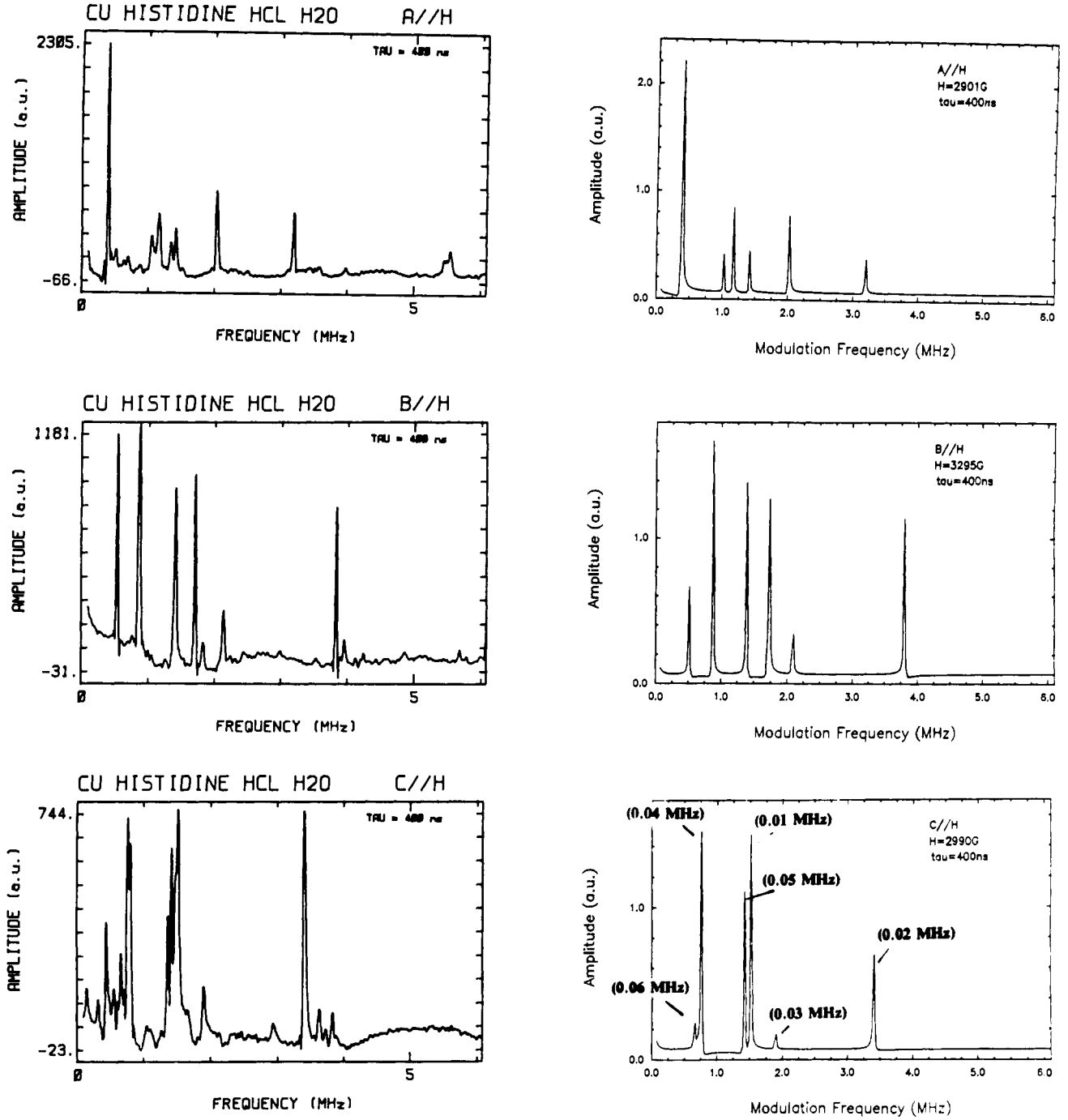

Figure 1. Left: Fourier transforms of the electron spin–echo envelope decay patterns (FT-ESEEM) acquired at orientations of the applied magnetic field (H) along the crystallographic (and reference) a, b, and c axes. Microwave frequencies and magnetic fields at resonance are the following: 9.1116 GHz and 2901 G at $a//H$, 9.1121 GHz and 3295 G at $b//H$, and 9.0239 GHz and 2990 G at $c//H$, respectively. Right: Corresponding FT-ESEEM at these same orientations determined theoretically from the tensors listed in Table I as described in the text. Values in parentheses assigned to lines at $c//H$ are maximum differences calculated for the various ^{14}N modulation frequencies in the copper nuclear spin manifolds. Frequency lines of small intensity that are attributed to minor copper species in the doped crystal have been ignored. These lines are made evident upon comparing the experimental and calculated FT·ESEEM spectra.

frequency lines as a function of applied field direction are illustrated in Figure 2.

The assignment of site split branches, like in the previous ligand ENDOR study,[16] was difficult because of the small site splittings of the various interaction tensors. The refined parameters corresponding to one possible set of tensors were rejected on the criterion that the quadrupole tensor principal directions should be as close to the molecular reference as was found by ENDOR for the quadrupole tensor of the imidazole ^{14}N directly bound to copper.[16] In addition, the site split branch of the g tensor in the ab plane was successfully correlated with the nitrogen lines by performing an ESEEM experiment at the field extrema of the EPR absorption while the field direction subtended a 45° angle with respect to the a axis. The remaining ambiguity in the correlation of the ^{14}N hyperfine and quadrupole tensors with the g tensor in regards to which symmetry related histidine molecule was therefore reduced to two possibilities.[30]

The data set consisted of 655 measured ESEEM modulation frequencies and resonant magnetic fields which were roughly distributed equally in three orthogonal planes. All data were assigned a weight of 1. The standard deviation in the data is 0.019 MHz. The final refined ^{14}N hyperfine and quadrupole coupling

(30) The g tensor (and therefore the copper hyperfine tensor) chosen to correlate with the ^{14}N ESEEM frequencies is related to the tensor given in Table I of McDowell et al.[16] by a 2-fold rotation about the b axis.

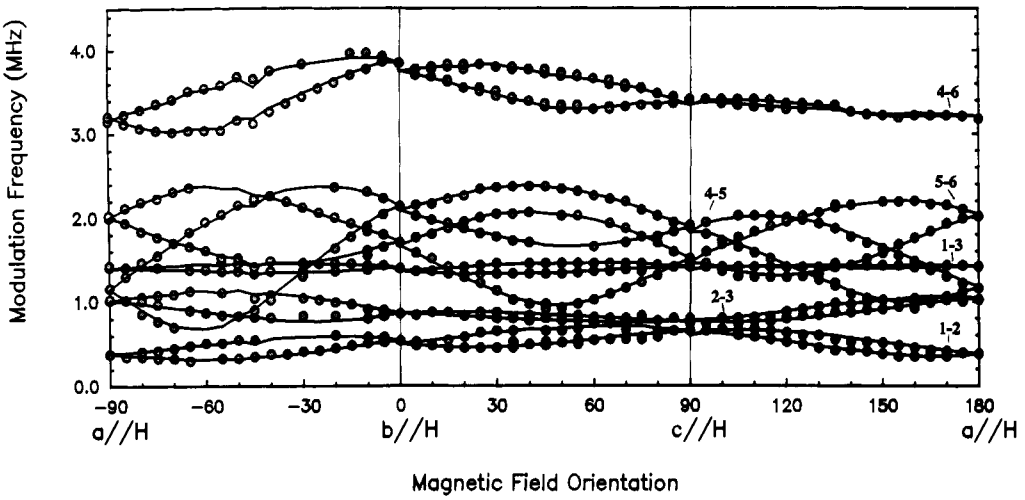

Figure 2. Angular dependencies of the observed ^{14}N modulation frequency lines in three planes defined by the *a*, *b*, and c reference axes. Frequencies are enumerated according to the spin energy level scheme in Figure 5 and ref 14. These frequency data were least-squares fit to the ^{14}N hyperfine and quadrupole tensor parameters as described in the text. Solid curves are calculated angular dependencies using tensors in Table I[30] and measured field magnitudes at discrete orientations. The slightly wavy nature in some regions of the plot is due to differing spectrometer operating frequencies (and resonant fields) that were utilized during the data collection.

tensors for one of the two possibilities of g-tensor correlation that was mentioned above are listed in Table I.[30] Standard deviations are 0.0037 MHz and <2° for the tensor principal values and directions, respectively. The solid curves in Figure 2 are calculated angular variations of the electron spin–echo modulation frequencies using the tensors in Table I and the experimental field magnitudes. In addition, FT-ESEEM simulations using the tensors in Table I are shown in the right panels of Figure 1.

Small splittings in some FT-ESEEM frequencies are consistently found when the applied field is aligned along the crystal *c* axis, i.e., *c*//*H*. The FT-ESEEM simulation at *c*//*H* has lines with intensities that are roughly equal to the combined split line intensities. McDowell et al. also observed split chlorine ENDOR frequencies at and near *c*//*H* which were attributed to an indirect nuclear spin–spin coupling between the chlorine and copper nuclei.[31] Measured ^{14}N ESEEM frequency line splittings at *c*//*H* are approximately equal to differences in the ^{14}N nuclear spin state transition frequencies in the various copper nuclear spin states which were calculated using tensors in Table I and the g and copper hyperfine tensors reported by McDowell et al.[16,30] The maximum splitting calculated for each of the nitrogen modulation frequencies *c*//*H* is given in parentheses in Figure 1. Apart from the disparity at *c*//*H*, very good correspondence is generally found between simulated and experimental spectra (see Figure 1).

The Hyperfine Coupling Tensor. As specified in Table I, the isotropic component of the remote ^{14}N hyperfine coupling tensor (a_{iso}) for copper-doped L-histidine HCl·H_2O is 1.35 MHz. This is slightly smaller than that recently found in Cu(II)-doped zinc(II) bis(1,2-dimethylimidazole) dichloride single crystal which had a_{iso} values of 1.42 and 1.37 MHz for the remote nitrogens of the two coordinated 1,2-dimethylimidazoles.[14] Aside from the bonding differences of the remote nitrogens in these two different molecules (i.e., >N–H versus >N–CH_3), a significant impact on the ^{14}N hyperfine interaction should also be expected in view of the very different copper unpaired orbitals postulated for these systems, predominantly dz^2 in the present system[15,16] versus predominantly $d(x^2-y^2)$ for doped zinc(II) bis(1,2-dimethylimidazole) dichloride.[19] In addition, the ligand arrangement around copper in the 1,2-dimethylimidazole system is a distorted tetrahedron[14,19] whereas the imidazole nitrogen ligand in L-histidine HCl·H_2O essentially defines the *z* axis.[15,16] The amount of spin delocalization on the copper bound ligand atoms appears to reflect these differences since single-crystal EPR measurements of the copper in zinc(II) bis(1,2-dimethylimidazole) dichloride suggest that nitrogen isotropic hyperfine couplings are about 20 MHz,[19] two-thirds that found by ENDOR measurements for the imidazole nitrogen in Cu(II)-doped L-histidine HCl·H_2O.[16] However, a comparable fractional change in the isotropic coupling of the remote nitrogen is not observed.

The form of the traceless part of the hyperfine tensor is essentially (*A*,0,–*A*) (0.37 MHz, –0.09 MHz, –0.28 MHz), with the –*A* direction deviating by only 8° and 3° from the imidazole plane normal direction and a quadrupole tensor principal direction, respectively. The other hyperfine tensor directions, although approximately in the imidazole plane, are not associated with any in-plane bonding directions. This form of anisotropy implies that the electron spin cannot be represented as a single point dipole. The total anisotropic value of 0.65 MHz is slightly higher than that found for the remote nitrogen coupling in Cu(II)-bound zinc(II) bis(1,2-dimethylimidazole) dichloride (0.53 MHz).[14] The tensor in the 1,2-dimethylimidazole system is, however, nearly axially symmetric (i.e., 2*A*, –*A*, –*A*),[14] which suggests a significant difference in the unpaired electron distributions in these two crystals.

The Quadrupole Coupling Tensor. The quadrupole coupling tensors for the histidine imidazole nitrogens (N2 and N3, see Figure 3) in L-histidine HCl·H_2O have been previously determined by single-crystal nuclear magnetic resonance (NMR) measurements.[7] In the present analysis, the sign choice for the quadrupole interaction is based on the assumption that the quadrupole tensor parameters for remote nitrogen in the copper-bound molecule will not be drastically different than those found in the undoped crystal. A comparison of Table I with Table 1 of ref 7 shows a close coincidence between the ESEEM quadrupole tensor directions and those measured by NMR for the imidazole N2 nitrogen (the angular deviations between the principal axes being 4°, 2°, and 4°). The ENDOR-measured N3 quadrupole tensor orientation in the copper-doped crystal,[16] on the other hand, shows a slightly larger misalignment from the NMR derived tensor (with angular deviations of 5°, 11°, and 11°). Overall, however, the good correspondences of the nitrogen quadrupole tensor principal orientations measured by ENDOR and ESEEM with the NMR tensor directions for the N3 and N2 nitrogens, respectively, suggest that the copper-coordinated imidazole moiety is not changed significantly compared to the structure of the molecule in the undoped crystal.

Comparing the tensor direction cosines in Table I with the L-histidine HCl·H_2O imidazole N2 reference directions[7] obtained from neutron diffraction results shows that, within the estimated uncertainty, the largest (0.70 MHz), smallest (–0.12 MHz), and intermediate (–0.58 MHz) quadrupole interactions for N2 lie along the perpendicular to the N2–H9 direction in the imidazole plane, along the N2–H9 bond direction, and along the normal to the imidazole plane, respectively. This is in contrast to that

(31) McDowell, C. A.; Sastry, D. L. *J. Chem. Phys.* **1988**, *89*, 2697.

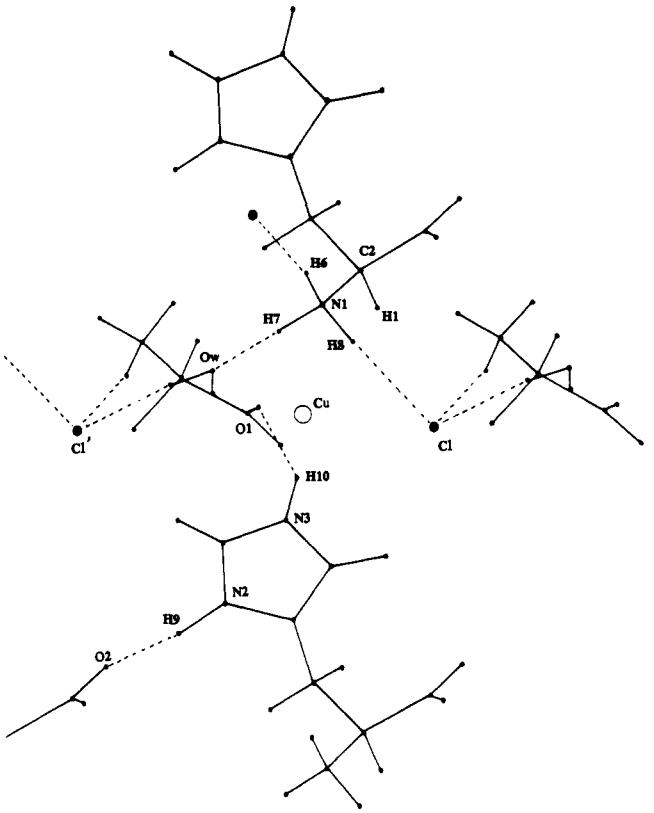

Figure 3. Postulated copper binding site in the crystal structure[25] of L-histidine HCl·H_2O. The copper position is at the midpoint of the amino group N1 of one histidine and the imidazole N3 of another (with Cu^{II}···N distances of 2.09 Å). Both nitrogens deprotonate upon copper ligation.[15,16] In addition, the copper makes contacts with chloride (Cl) and oxygens from water (Ow) and carboxylate (O1). Magnetic coupling interactions between the unpaired electron and the imidazole N2 nitrogen (or remote nitrogen) are the subject of the present investigation. Hydrogen-bonding interactions are depicted by the dotted lines.

found for the remote nitrogen tensor in Cu(II)-doped zinc(II) bis(1,2-dimethylimidazole) dichloride where the largest quadrupole interaction (−1.12 MHz) is normal to the imidazole plane, the intermediate value (0.63 MHz) is along the N–CH_3 bond direction, and the smallest coupling interaction (0.49 MHz) is perpendicular to both the N–CH_3 and plane normal directions.[14] It has been suggested that the reorientation of the direction of largest quadrupole coupling (see II) reflects major differences in the nitrogen bonding features of imidazole compounds.[4,5,8]

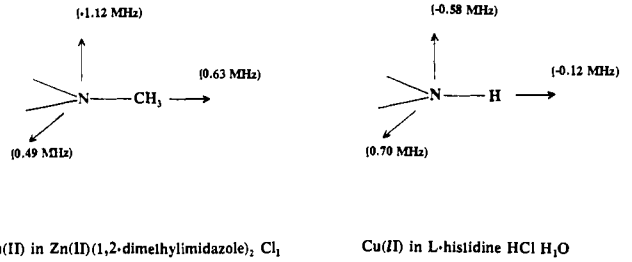

Cu(II) in Zn(II)(1,2-dimethylimidazole)$_2$ Cl_2 Cu(II) in L-histidine HCl H_2O

II

A Townes–Dailey analysis[10,32] using the formal charge modification given by Gordy and Cook[33] was undertaken. The usual scheme for imidazole nitrogen hybrid orbitals was employed to describe the bonding arrangement.[10] The ring C–N nitrogen valence orbital occupancy, *B*, was assigned a value of 1.142, being based on a normalizing condition that the imino nitrogen of imidazole in L-histidine is assigned a lone pair occupancy of 2. It was further assumed, as has been done previously,[1,34] that the imidazole ring C–N occupancy be the same for all compounds in the analysis.

Table II. Results of a Townes–Dailey Analysis[32,33] of the ^{14}N Quadrupole Parameters in a Series of Imidazole-Containing Molecules[a]

compd	valence occupancies *A*	*B*	*C*	charge
L-histidine HCl·H_2O				
$N_\epsilon(3)$–H	1.301	1.142	1.306	0.0999
$N_\delta(2)$–H	1.415	1.142	1.302	−0.0100
Cu(II) in L-histidine HCl·H_2O				
$N_\epsilon(3)$–Cu	1.610	1.142	1.222	−0.1247
$N_\delta(2)$–H	1.362	1.142	1.312	0.0333
L-histidine				
N_ϵ–H	1.334	1.142	1.327	0.0462
N_δ	2.000	1.142	1.109	−0.4016
1,2-dimethylimidazole				
N–CH_3	1.079	1.142	1.349	0.2793
Cu(II) in Zn^{II}(1,2-dimethylimidazole)$_2Cl_2$				
N–CH_3	1.105	1.142	1.329	0.2727
	1.103	1.142	1.343	0.2608

[a] The *C*, *B*, and *A* occupancies refer to the ^{14}N valence populations associated with the ^{14}N hybrid orbitals[10] with axes normal to the imidazole plane, along the ring C–N bonds, and along the N–H (or N–CH_3 or N···Cu^{II}) bond, respectively. Nitrogen quadrupole tensor parameters were obtained from single-crystal NMR for L-histidine HCl·H_2O,[7] powder NQR for L-histidine(orthorhombic)[13,35] and 1,2-dimethylimidazole,[3] a previous single-crystal ESEEM analysis of Cu(II)-doped zinc(II) bis(1,2-dimethylimidazole) dichloride,[14] an ENDOR study for the copper-bound imidazole N3 in L-histidine HCl·H_2O,[16] and the present work for the imidazole N2 in Cu(II)-doped L-histidine HCl·H_2O. The quadrupole tensor orientations were assumed in the analysis of the imino and amino nitrogens of imidazole in L-histidine(orthorhombic) and of the amino nitrogen in 1,2-dimethylimidazole.

The *C* and *A* populations refer to the valence occupancies associated with the nitrogen orbitals normal to the imidazole plane and along the N–H (or N–Cu or N–CH_3) bond, respectively. Results are listed in Table II for quadrupole interactions at N2 and N3 in L-histidine HCl·H_2O obtained from NMR,[7], ENDOR,[16] or ESEEM, at the amino nitrogen in 1,2-dimethylimidazole[3] and at both imidazole nitrogens in L-histidine(orthorhombic)[13,35] as determined from powder NQR, and at the remote nitrogens in Cu(II)-doped zinc(II) bis(1,2-dimethylimidazole) dichloride from ESEEM measurements.[14] The assignment of tensor principal values to their respective directions has been assumed for the NQR powder results. Uncertainties in occupancy values derived from ESEEM results have been estimated to be ≈0.0006 electron units, and similar standard deviations for listings in Table II are expected. The relevant features in Table II are the following:

(a) There is a significant difference in the *A* populations for the two nitrogens (N2 and N3) in L-histidine HCl·H_2O which may be partially due to their molecular inequivalence. Ab initio calculations performed on the L-histidine molecule in L-histidine HCl·H_2O predicted differences in imidazole nitrogen quadrupole parameters.[8] Further calculations using formate ions as a model for the hydrogen-bonding interactions in this crystal, although giving better agreement with the experimental results, failed to reconcile the large quadrupole variation observed.[8] McDowell et al.[7] also concluded that the difference in quadrupole parameters for the two imidazole nitrogens in L-histidine HCl·H_2O was a consequence of intermolecular hydrogen bonding (the crystal structure shows significantly different hydrogen-bonding interactions for the two imidazole nitrogens, with >N2–H9···O2 and >N3–H10···O1 distances of 1.580 and 1.941 Å, respectively[25]).

(32) Townes, C. H.; Dailey, B. P. *J. Chem. Phys.* **1949**, *17*, 782.
(33) Gordy, W.; Cook, R. L. In *Chemical Applications of Spectroscopy Part III: Molecular Spectra*; West, W., Ed.; John Wiley and Sons: New York, 1970; Chapter 14.
(34) Hiyama, Y.; Butler, L. G.; Olsen, W. A.; Brown, T. L. *J. Magn. Reson.* **1981**, *44*, 483.
(35) Edmonds, D. T.; Summers, C. P. *J. Magn. Reson.* **1973**, *12*, 134.

(b) When copper binds to the N3 nitrogen of imidazole in L-histidine HCl·H_2O it causes a large change in its *A* occupancy. The N3 *C* population decreases for the copper-bound as compared to the protonated histidine, most likely as a response to the large increase in the *A* population. The nitrogen formal charge becomes more negative apparently because of the less positve charge transfer to nitrogen from the copper as compared to the proton.

(c) The change of valence populations for the remote nitrogen (N2) in L-histidine HCl·H_2O upon copper binding is, as expected, not as dramatic as the changes occurring at the N3 nitrogen. A significant decrease in the *A* occupancy does however occur in the copper-coordinated as compared to the protonated imidazole. This occupancy change is in the opposite direction compared to changes at N3, that is, as the imidazole moiety becomes more negative, the N2 *A* occupancy decreases and also the net formal charge at N2 becomes more positive. A similar change is seen for the case of 1,2-dimethylimidazole where, even though the relative occupancies are very different than in the histidine molecules, the *A* occupancy of the remote nitrogen increases upon copper coordination.

Discussion

The present results indirectly confirm the coordination of the ϵ nitrogen (N3) of histidine to the doped copper ion by characterizing the magnetic coupling parameters of the δ nitrogen (N2). The strongest support for the remaining ligand nuclei comes from the previous ENDOR analysis.[16] Positioning the copper ion at the midpoint of the N1 and N3 nitrogens from two ligating histidines results in reasonable ligand contact distances (e.g., distances to Cu(II) from both N1 and N3 are 2.09 Å) and good correlations with the previously obtained **g**, copper, and ligand tensor orientations[16,30] without the need to reorient the atoms from the positions defined by the crystal structure studies.[24,25] The postulated copper-doping site in the crystal structure of L-histidine HCl·H_2O is illustrated in Figure 3. Here the copper site is also interstitial to chloride (Cl), carboxyl oxygen (O1), and water (Ow). This model is consistent with present results which show a very good correlation between the N2 quadrupole tensor orientation with respect to the imidazole moiety unperturbed from its crystal structure position.

A simple hyperfine tensor calculation using a multipoint representation of the electron spin density in the copper dz^2 orbital (two points of 0.30 fraction electron spin each at a distance of 1 Å on either side of the postulated copper position along the minimum **g** value direction, i.e., approximately ≈5° from the vector joining Cu and N3) and in the N3 $2p_x$ orbital (two points of 0.045 fraction electron spin each at a distance 0.5 Å on either side of N3 along the direction of the presumably absent N3–H10 bond) gives good agreement with the previous ENDOR measurements[16] both in magnitude (the experimental and calculated maximum components of the anisotropic part of the nearly axial tensor are 5.87 and 5.94 MHz, respectively) and direction (the deviation between the calculated and experimental directions associated with these couplings is 2°). From this estimated spin density distribution on the copper and imidazole N3, and including at the position of N3 the fraction 2s electron spin density, ≈31.83 MHz/1540 MHz (with 31.83 MHz being the isotropic component of the N3 hyperfine tensor from ENDOR measurements and 1540 MHz being the ^{14}N isotropic coupling of an unpaired electron completely occupying the nitrogen 2s atomic orbital),[36] the anisotropic hyperfine components of N2 were evaluated by further assuming that the fraction 2s unpaired spin character of ≈1.35 MHz/1540 MHz at N2 arises from equal contributions of the three N2 hybrid orbitals in the imidazole plane. The N2 hyperfine tensor anisotropic components so calculated have principal components of 0.27, −0.07, and −0.20 MHz with deviations from the experimental directions of 6°, 9°, and 6°, respectively. Thus a scheme for spin density delocalized over the copper and imidazole moiety is put forth that gives good estimates for both the N2 and N3 hyperfine tensors. The existence of a reasonable representation of spin density further supports the model suggested above.

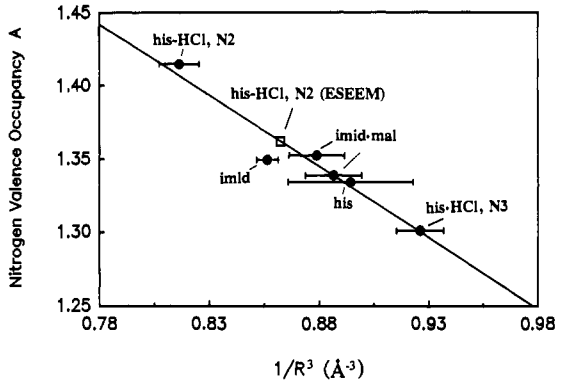

Figure 4. Plot illustrating the linear dependence of ^{14}N valence occupancy *A* determined by a Townes–Dailey analysis on the inverse cube of the corresponding imidazole amino N–H bond lengths for a series of compounds. The compounds included in the analysis (L-histidine(orthorhombic) (his), imidazole (imid), L-histidine HCl·H_2O (his-HCl), and imidazolium hydrogen maleate (imid-mal)) are those that have been the subject of both neutron diffraction (his,[38] imid,[39] his-HCl,[25] imid·mal[40]) and NMR (his·HCl[7]) or NQR (his,[13,35] imid,[5] imid·mal[41]) studies. The nitrogen quadrupole tensor axis orientations are assumed in the analysis of the parameters for L-histidine(orthorhombic), imidazolium hydrogen maleate, and imidazole. The open square represents the predicted position for the imidazole N2 nitrogen in Cu(II)-doped L-histidine HCl·H_2O using the *A* occupancy derived from ESEEM results. Error bars represent standard deviations in the derived quantities.

Previous magnetic resonance studies have resulted in an unambiguous assignment of the ^{14}N quadrupole tensor orientations of the imidazole nitrogens of L-histidine HCl·H_2O,[7] of the directly bound imidazole nitrogen in the copper-doped form of this system,[16] and of the remote nitrogens of the two coordinated 1,2-dimethylimidazoles in copper-doped zinc(II) bis(1,2-dimethylimidazole) dichloride.[14] Also it has been shown that the remote nitrogen quadrupole tensor, rather than the hyperfine interaction, is a key identifying parameter in copper-bound imidazole complexes.[14] Results from the present work are consistent with these findings.

A series of imidazole-containing molecules[37] that have both been the subject of neutron diffraction studies[25,38-40] and had their imidazole amino nitrogen quadrupole parameters determined by either single-crystal NMR[7] or NQR[5,13,35,41] were analyzed by the Townes–Dailey approach as outlined above. The nitrogen *A* occupancies so determined were plotted as a function of the inverse cube of the corresponding N–H bond lengths. Results are displayed in Figure 4 where a very good correlation is seen. Similar empirical dependencies have been found for deuterium quadrupole parameters in O–D···O,[41,42] N–D···O,[1,43,44] and N–D···H[6] systems. However, given the paucity of data, the observed trend shown in Figure 4 must be considered as only tentative. Nevertheless, if the N2 nitrogen *A* population determined from the present study is placed on the line in Figure 4, the relationship predicts that the N2–H9 bond length decreases by ≈0.02 Å as compared to that of the undoped crystal structure. Empirical dependencies such as that illustrated in Figure 4 have the potential to accurately

(36) Reference 29, Table C.

(37) Molecules included in the analysis are imidazole, L-histidine(orthorhombic), L-histidine HCl·H_2O, and imidazolium hydrogen maleate. References for the specific crystal structures and quadrupole parameters are given in Figure 4.

(38) Lehmann, M. S.; Koetzle, T. F.; Hamilton, W. C. *Int. J. Peptide Protein Res.* **1972**, *4*, 229.

(39) McMullan, R. K.; Epstein, J.; Ruble, J. R.; Craven, B. M. *Acta Crystallogr.* **1979**, *B35*, 688.

(40) Hussain, M. S.; Schlemper, E. O.; Fair, C. K. *Acta Crystallogr.* **1980**, *B36*, 1104.

(41) Poplett, I. J. F.; Sabir, M.; Smith, J. A. S. *J. Chem. Soc., Faraday Trans. 2* **1981**, *77*, 1651.

(42) Soda, G.; Chiba, T. *J. Chem. Phys.* **1969**, *50*, 439.

(43) Hunt, M. J.; Mackay, A. L. *J. Magn. Reson.* **1976**, *22*, 295.

(44) Reuveni, A.; Marcellus, D.; Parker, R. S.; Kwiram, A. L. *J. Chem. Phys.* **1981**, *74*, 179.

predict small variations in N-H bond lengths in imidazole systems solely from the ^{14}N quadrupole tensor parameters. In addition, the aforementioned opposing changes that occur in the A occupancies of the imino and amino imidazole nitrogens are consistent with the hypothesized decrease in N2-H9 bond length upon copper binding. As the imidazole moiety becomes more negative on going from the protonated to the copper-bound forms, the amino N_δ-H bond lengths become progressively shorter. Thus as the strength of the N-H bond increases, the valence A occupancy decreases and with it a concomitant positive increase in the nitrogen net formal charge.

Conclusions

The hyperfine tensor of the imidazole remote nitrogen of histidine has been accurately determined by ESEEM in Cu(II)-doped L-histidine $HCl \cdot H_2O$ single crystals. The tensor anisotropy exhibits a non-axial form as compared to the axial hyperfine tensor found for the remote nitrogen in Cu(II)-doped zinc(II) bis(1,2-dimethylimidazole) dichloride.[14] Unlike this previous ESEEM study, the nitrogen hyperfine tensor in the Cu(II)-doped L-histidine $HCl \cdot H_2O$ system could be reasonably modeled by a simple multipoint representation of the unpaired electron distribution which is delocalized to a small extent from the metal to the imidazole moiety. It is thus difficult to predict the situations where axial or non-axial hyperfine tensors are expected.

Minor spin delocalization in a $Cu^{II}(imidazole)_4$ complex has been previously inferred from the observation of finite isotropic hyperfine components of the imidazole remote nitrogen (by ESEEM[45] and ENDOR[46]) and protons (by ENDOR[46]) in frozen solution studies. The isotropic component of the nitrogen hyperfine tensor in the present system is only slightly smaller than that recently determined in a single-crystal ESEEM analysis of copper doped into the tetrahedral metal site of zinc(II) bis(1,2-dimethylimidazole) dichloride.[14] It appears that this component of the hyperfine interaction is not as sensitive an indicator of copper coordination geometry, and of the postulated metal unpaired orbital, as in the form of the tensor anisotropy. Future studies of similar systems may help evaluate this hypothesis.

The quadrupole tensor for N2 was likewise determined by the single-crystal ESEEM measurements. A good correlation was found between this tensor orientation and the imidazole geometry. This observation in conjunction with calculated estimates of the hyperfine tensor for both imidazole nitrogens indicate that, upon copper ligation, the imidazole moiety does not distort from its position in the crystal structure[24,25] to a degree that is significant within the accuracy of the ESEEM results.

The variations observed in the quadrupole parameters of the remote nitrogen of imidazole of coordinated histidine derived from ESEEM of frozen solution protein samples have been postulated to be the consequence of intermolecular hydrogen-bonding differences.[9,23f] N—H bond lengths and N—H···O=C distances have been roughly correlated by previous crystallographic analysis.[47] Ab initio calculations have shown that the inequivalence of the two imidazole nitrogens in L-histidine $HCl \cdot H_2O$ may also be a factor in the observed quadrupolar variations.[4] Both intramolecular and intermolecular interactions should affect the remote nitrogen N-H bond length. A linear relationship is found between the A valence population of imidazole amino nitrogens and the inverse cube of the corresponding N-H bond lengths in a series of model compounds. Such an empirical dependence has the potential for deducing the N-H bond lengths in imidazole-containing molecules from the analysis of ^{14}N quadrupole tensor parameters.

Acknowledgment. M.J.C. thanks Dr. Jacqueline Vitali for helpful discussions. This work was supported by U.S.P.H.S. Grants RR-02583 and GM-40168 to J.P.

(45) Mims, W. B.; Peisach, J. *J. Chem. Phys.* **1978**, *69*, 4921.
(46) Van Camp, H. L.; Sands, R. H.; Fee, J. A. *J. Chem. Phys.* **1981**, *75*, 1098.
(47) Traylor, R.; Kennard, O.; Versichel, W. *Acta Crystallogr.* **1984**, *B40*, 280.

Normal Modes and NMR Order Parameters in Proteins

Rafael Brüschweiler†

Contribution from the Laboratorium für Physikalische Chemie, ETH Zentrum, 8092 Zürich, Switzerland. *Received December 27, 1991*

Abstract: On the basis of a normal-mode analysis of the protein BPTI, it is demonstrated that the very fast time scale backbone motions with correlation times much faster than 100 ps have a measurable influence on both homonuclear and heteronuclear NMR relaxation rates. Significant differences between classical and quantum statistics are found for heteronuclear relaxation.

1. Introduction

Nuclear magnetic relaxation spectroscopy[1] is one of few experimental sources providing spatially resolved information on sub-nanosecond dynamics of biomolecules in solution. Dipolar relaxation data (T_1, $T_{1\rho}$, T_2, and NOE) of heteronuclear spin pairs, such as ^{13}C-H and ^{15}N-H, are often interpreted using the Lipari-Szabo model,[2] where the motion of the involved internuclear vector is characterized by an internal time scale τ_e, an overall time scale τ_c, and an order parameter S^2. Recently, Clore et al.[3] extended the Lipari-Szabo model by the introduction of an additional order parameter S_f^2, which characterizes the spatial extent of very fast time scale motions ($\tau_e \ll 100$ ps) such as atomic fluctuations and vibrations. The results in ref 3 show that, for most parts of the backbone of the investigated protein (interleukin β), the dominant contribution to the total order parameter S^2 is given by S_f^2 (exceptions are mobile loop regions).

The experimental accessibility of S_f^2 is interesting from a theoretical point of view, since it allows a direct atom-site-specific comparison between analytical as well as force-field-based molecular motional models and NMR data. In the present con-

†Present address: Department of Molecular Biology, The Scripps Research Institute, 10666 North Torrey Pines Rd., La Jolla, CA 92037.

(1) Abragam, A. *Principles of nuclear magnetism*; Clarendon Press: Oxford, England, 1961.
(2) Lipari, G.; Szabo, A. *J. Am. Chem. Soc.* **1982**, *104*, 4546.
(3) (a) Clore, G. M.; Szabo, A.; Bax, A.; Kay, L. E.; Driscoll, P. C.; Gronenborn, A. M. *J. Am. Chem. Soc.* **1990**, *112*, 4989. (b) Clore, G. M.; Driscoll, P. C.; Wingfield, P. T.; Gronenborn, A. M. *Biochemistry* **1990**, *29*, 7387.

0002-7863/92/1514-5341$03.00/0